



Trade Science Inc.

# Materials Science

An Indian Journal  
Full Paper

MSAIJ, 4(4), 2008 [297-305]

## A metallographic study of several alloys and of their pre-solder and post-solder joints used in dental prostheses

Pascal De March<sup>1,2</sup>, Patrice Berthod<sup>2\*</sup>

<sup>1</sup>Faculte d'Odontologie de Nancy, Département de Prothèses, 96 avenue de Lattre de Tassigny,  
B.P. 50208, 54000 Nancy, (FRANCE)

<sup>2</sup>Laboratoire de Chimie du Solide Minéral (UMR 7555), Faculté des Sciences et Techniques,  
UHP Nancy 1, Nancy-Université, B.P. 239, 54506 Vandoeuvre-les-Nancy, (FRANCE)

E-mail: Patrice.Berthod@lcsm.uhp-nancy.fr

Received: 16<sup>th</sup> May, 2008 ; Accepted: 21<sup>st</sup> May, 2008

### ABSTRACT

Prosthesis frameworks are usually the assemblage of successive alloys. One of them can present a mechanical weakness, e.g. due to internal defects, which can cause an untimely rupture. The aim of this study is to perform metallographic investigations on several parent alloys and pre- and post-solders in order to reveal a possible heterogeneity of properties, as well as to number the metallurgical phenomena that may locally weaken a framework in real situation. Eight parent alloys belonging to three different classes were investment cast. Two pieces of a same parent alloy were soldered together and the assemblage underwent a heat treatment. Internal metallurgical health and microstructure of both alloy and solder were studied and their microhardness was measured. Internal defects were noticed in several parent alloys and solder joints, inside samples which reproduce real conditions of use. The microstructures of all parent and solder alloys were characterized, as well as the inter-diffusion zone. The pre-soldering leads to an inter-diffusion which is more extended than for post-soldering, due to a higher soldering temperature. The composition and the microstructure of the solder joint are not changed in a main part of its thickness, and its microstructure remains different from the parent alloy's one.

© 2008 Trade Science Inc. - INDIA

### KEYWORDS

Fixed partial denture;  
Dental alloys;  
Soldering;  
Microstructure;  
Diffusion;  
Hardness.

### INTRODUCTION

Soldering, which pools well-known means to butt-joint two metallic pieces<sup>[1,2]</sup>, is notably well used to join sections of conventional fixed partial denture (Figure 1). This allows correcting the distortion of the framework during the casting process<sup>[3]</sup>, improving the seating accuracy<sup>[4]</sup> and correcting the movement of teeth occurred before the prosthesis cementation<sup>[5]</sup>. One of the major causes of failure in a fixed partial denture is related to

the mechanical resistance of the metallic framework

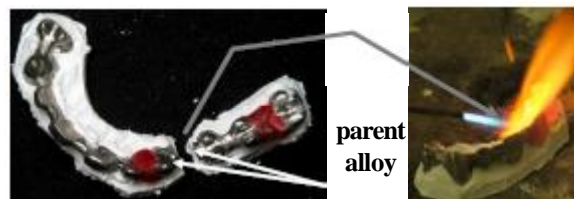


Figure 1: Example of soldering of two parts of the metallic framework (parent alloy) for a dental prosthesis

## Full Paper

TABLE 1: Chemical compositions of the studied parent alloys (in wt.%; manufacturer's data)

Elements	Au	Pt	Pd	Ag	Ga	In	Re	Ru	Sn	Zn	Others
<b>"High Noble" alloys (for which Au+Pt+Pd &gt; 60wt.%) *</b>											
IPS dSIGN98	85.9	12.1	-	-	-	<1.0	-	-	-	2.0	In <1 Ir <1 Fe <1 Mn <1 Ta <1
IPS dSIGN91	60.0	-	30.6	-	1.0	8.4	<1.0	<1.0	-	-	-
Aquarius Hard	86.1	8.5	2.6	-	-	1.4	-	<1.0	-	-	Fe <1 Li <1 Ta <1
Lodestar	51.5	-	38.5	-	1.5	8.5	<1.0	<1.0	-	-	-
W	54.0	-	26.4	15.5	-	1.5	<1.0	<1.0	2.5	-	Li <1
<b>"Noble" alloy (containing Au+Pt+Pd) *</b>											
IPS dSIGN59	-	<1.0	59.2	27.9	-	2.7	<1.0	<1.0	8.2	1.3	Li <1
Elements	Ni	Cr	Mo	Al	Si	W	Others				
<b>"Predominantly Base" alloys (containing less than 25wt.% Au+Pt+Pd) *</b>											
Pisces plus	61.5	22.0	-	2.3	2.6	11.2	Mischmetal <1				
4all	61.4	25.7	11.0	<1	1.5		Mn <1				

\*: Identalloy® norm

which supports the visible external ceramic. This is notably influenced by the mechanical properties of the solder joint which can be considered as being the weakest part of the framework<sup>[6,7]</sup>. This explains why the mechanical behavior of different solder joints were evaluated in previous studies<sup>[8-10]</sup>, especially to determine the influence of structure defects. The microstructure characterizations of the parent alloys and of their solder joints are known as being determinant means for the prediction of the mechanical resistance of fixed partial prostheses<sup>[11,12]</sup>. In this work metallographic investigations of the microstructures of several selected alloys and of their corresponding pre-ceramic and post-ceramic solders, completed by micro-hardness measurements, are performed in order to identify the possible metallurgical characteristics which can threaten the good behavior of a fixed prosthesis using these alloys in its framework.

## EXPERIMENTAL

### The studied alloys

Eight parent alloys (five rich in noble elements and called "High Noble", one with lower contents in noble elements and called "Noble" and two (Ni,Cr)-based alloys called "Predominantly Base", in conform with the Identalloy® norm) and their corresponding pre- and post-solder alloys, were investigated. TABLES 1-3, indicate respectively the compositions of the parent alloys, the compositions of the solders, and how the parent alloy and the solder alloy must be associated to each other as indicated by the manufacturer.

The parent alloys were realized by investment casting. A pattern resin was injected in a machined metallic

TABLE 2: Compositions of the studied solder alloys (in wt.%; manufacturer's data)

Pre-solder	Au	Pd	Ag	In	Ni	Others	
HGPKF 1015 Y	60.0	-	36.5	<1.0	-	Pt <2.1 Ir <1 Sn <1 Zn <1	
SHFWC	47.0	10.3	41.0	1.4	-	Ru <1	
HFWC	45.0	12.4	41.5	1.0	-	Ru <1 Li <1	
Super solder	-	53.5	7.0	-	35.6	Sn = 3.8 Li <1	
Post-solder	Au	Ag	Cu	Ga	In	Sn	Zn
0.650 Gold Solder	65.0	13	19.6	2.0	-	-	<1.0
0.615 Fine Solder	61.3	13.1	17.4	-	7.6	-	<1.0
0.585 Fine solder	58.5	16.0	18.0	7.2	-	-	<1.0
LFWG	56.1	27.4	-	-	<1.0	<1.0	15.8

mold, in order to obtain the models which thereafter allowed obtaining the final mold in which the liquid parent alloy was finally injected using a casting machine with a centrifugal arm (Minicast®, Uger) and a gas-oxygen torch. All samples were then separated from the cast-rod.

### Preparation of the pre-ceramic solder samples

For each alloy, one sample of 10×10×1 mm<sup>3</sup> was cut into two equal pieces (5×10×1 mm<sup>3</sup>) with a diamond blade with a slow-speed precision saw (Isomet 5000, Buelher®). Each sample was blasted with Al<sub>2</sub>O<sub>3</sub> powder 50 μm (Blaster Harnish+Rieth and alumina powder Windent conform to norm FEPA 42F-1984). The soldering gap of 0.2mm<sup>[13]</sup> was obtained by interposing a 0.2mm thick paper between the two sectioned pieces which are firmly clamped with a sticky wax, before investment (Sodervest Quick GC). Paper and wax were also eliminated under a thread of warm water. Investment was dehydrated at ambient temperature and high fusing bondal flux (Williams®) was applied to the joint.

The pre-ceramic soldering was realized for each alloy with its corresponding solder as indicated in TABLE

**TABLE 3: Alloy-solder associations according to the manufacturer**

Alloy	Pre-solder	Post-solder
IPS d.SIGN 98	HGPKF 1015 Y	0.585
IPS d.SIGN 91	SHFWC	0.615
Aquarius hard	HGPKF 1015 Y	0.650
Lodestar	HFWC	0.615
W	HFWC	LFWG
IPS d.SIGN 59	SHFWC	0.615
Pisces plus	Super solder	LFWG
4all	Super solder	LFWG

**TABLE 4: The thermal cycles which were applied (according to IPS dSIGN, Ivoclar Vivadent®)**

Alloys	Oxidation
IPS d.SIGN 98	925°C/5 min/no vacuum
IPS d.SIGN 91	1010°C/5 min/under vacuum
Aquarius Hard	925°C/5 min/no vacuum
Lodestar	1010°C/5 min/under vacuum
W	1010°C/5 min/under vacuum
IPS d.SIGN 59	1010°C/10 min/no vacuum
Pisces Plus	1010°C/5 min/under vacuum
4all	950°C/1 min/no vacuum

Type of heat treatment	Temperatures		Heating rate	Stage duration	Temperatures (vacuum)	
	Baking	Service			Beginning	End
1 <sup>st</sup> opaque	900°C	403°C	80°C/min	1min	450°C	899°C
2 <sup>nd</sup> opaque	890°C	403°C	60°C/min	1min	450°C	889°C
Dentine I and 2	870°C	403°C	60°C/min	1min	450°C	869°C
Glazing	830°C	403°C	60°C/min	1min	450°C	869°C

3, with a gas-oxygen torch (butane-oxygen) respecting the manufacturer's technical advices. The solder joints were machined with a diamond separating disk, while the excess of solder was removed in order to obtain a smooth surface of sample. The soldered samples were sandblasted with 50µm alumina oxide and steam cleaned. The thermal cycle required for the respective "oxidation" heat treatment of each alloy was done in a ceramic oven (Programat X2, Ivoclar Vivadent®). All thermal cycles were realized according to the manufacturer's advices for IPS dSIGN® ceramic (Ivoclar Vivadent®), as following: "opaque wash", "opaque", "dentine baking I", "dentine baking II", and "glazing". These thermal conditions are reported in TABLE 4.

### Preparation of the post-ceramic solder samples

The same thermal cycles as previously described in TABLE 4 (oxidation, opaque wash, opaque, dentine bake I, dentine bake II, glazing), were realized in ceramic oven for two cast samples of 5×10×1 mm<sup>3</sup> which were destined to post-ceramic solder. Two individual samples were blasted and invested as previously described (Sodervest Quick, GC®) with a soldering gap

of 0.2mm gauged with a calibrated paper. Low-fusing bondal flux (Williams®) was applied to the joint, a piece of the corresponding solder was inserted in the soldering gap, and the post-ceramic soldering was realized in the ceramic oven (Programat X2 Ivoclar-Vivadent®) in conform with the manufacturer's advices for each solder. The excess of solder was eliminated, samples were sandblasted and steam cleaned like the pre-ceramic solder samples.

Unfortunately the post-ceramic solders were not possible for the two Ni-Cr alloys in conventional conditions with a soldering temperature matching with the firing temperature of ceramic 50°C (122°F) under 830°C (1,526°F), and the glazing temperature of IPS dSIGN® ceramic.

### Preparation of samples and metallographic analysis

All the prepared samples were cut into two parts using a precision saw (Isomet 5000, Buelher®) perpendicular to the solder joint. The two parts of the cut solder were both maintained by a titanium support and embedded in araldite resin (Escil®). The surface of interest was prepared for metallographic analysis by wet abrasion with SiC paper from grade 240 to 1200. They were then polished with 1µm diamond pastes. To prevent any pollution the samples were finally cleaned in ethanol with ultrasounds during three minutes.

The samples were observed using an optical microscope (Olympus® Vanox) and a scanning electron microscope (SEM), in back scattered electrons mode (BSE) for observing microstructures, and in secondary electrons mode (SE) for appreciating the surface relief. A microprobe (model SX100, Cameca Instruments Inc.) was used for wavelength dispersion spectrometry (WDS) measurements of chemical compositions, pin-point measurements for identifying the phases belonging to an alloy or a solder, or contents profiles through the interface between a parent alloy and a solder joint for characterizing the interdiffusion of the two alloys.

### Vickers microhardness measurements

Vickers micro hardness measurements were performed on each parent alloys, each pre-solder joint and each post-solder joint, using a Reichert D32 apparatus under a load of 32g. Three indentations were done,

## Full Paper

leading to an average value and a standard deviation value.

### RESULTS AND DISCUSSION

#### Internal metallurgical health of the parent alloys and of their solder joints

Figure 2 presents two SEM micrographs revealing two types of defects which can be found in the alloys and solders which were realized. TABLE 5 summarizes all the internal healthy problems which were met in all parent alloys and solders. If some alloys did not contain any internal defects, the other ones showed different internal healthy problems as micro-shrinkage defects (due to the alloy contraction during its solidification). These ones were more or less numerous, large or homogeneously dispersed in the whole thickness of the sample. The alloys are nevertheless quite preserved from

**TABLE 5: Internal metallurgical health of all alloys and of their pre-solder (I) and post-solder (II) joints**

Alloy Pre-solder joint (I) Post-solder joint (II)	Internal defects in the alloys	Internal defects in the pre-solder joint		Internal defects in the post-solder joint	
	Microshrinkage defects	Mic. shrink. defects	Porosities	Mic. shrink. defects	Porosities
<b>HN and N alloys</b>					
All. : IPS dSIGN98					
(I): HGPKF 1015 Y (II): .585	M2 M1	M2	P1	M1	P3
All. : IPS dSIGN91					
(I): SHFWC (II): .615	M2-3 M2	M3	/	M1	P2
All. : Aqua. Hard					
(I): HGPKF 1015 Y (II): .650	M0-1 /	M2	/	M0-1	P3
All. : Lodestar					
(I): HFWC (II): .615	M1-2 /	M0-1	P1	M0-1	P0-1
All. : W					
(I): HFWC (II): LFWG	M1-2 /	M1	/	M2	P2
All. : IPS dSIGN59					
(I): SHFWC (II): .615	M0-1 /	M0-1	/	M2	/
<b>PB alloys</b>					
All. : Pisces plus					
(I): Super solder (II): LFWG	M0-1 *	M2	/		*
All. : 4ALL					
(I): Super solder (II): LFWG	/ *	M1	/		*

Significations of the codes used above: (M0) M1, M2, M3: no micro-shrinkage defects (/ or M0), rare (1), numerous (2), very numerous (3), P0, P1, P2, P3: no porosities (0), small (1), medium size (2), enormous (3), \*: post-soldering was impossible

porosities. Most of the pre-ceramic solders present micro-shrinkage defects but no visible porosities.

Inversely, several post-ceramic solders present very big porosities, which could be sometimes lacks, as is to say other casting defects resulting from a not totally achieved filling of the gap before that solidification acts and obstructs it. Otherwise, two post-ceramic solder were impossible to realize. Indeed, the two Predominantly Base alloys (Pisces Plus and 4ALL, which are both (Ni, Cr)-based alloys), which could have been brazed in high temperature by gas-oxygen torch with a primary (Pd, Ni)-based solder alloy (Super Solder®), were unable to be brazed at lower temperature (post-ceramic solder in ceramic oven) with an (Au, Ag)-based alloy solder.

#### Microstructure of the alloys

Most of the alloys display two distinct phases. Indeed, seven on the eight present a matrix and precipitates which are either clearer or darker than matrix when observed with the SEM in BSE mode. Figure 3 presents micrographs of the parent alloys microstructures and figure 4 shows the microstructures of the pre-and

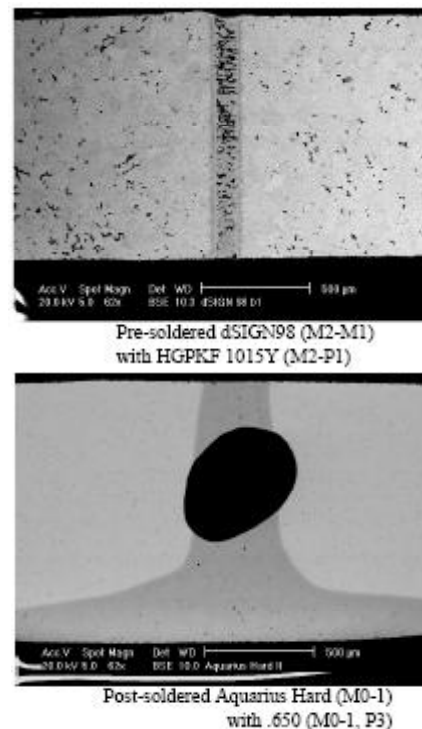


**Figure 2: Internal metallurgical defects in an alloy (micro-shrinkage defects, left hand), in a pre-solder joint (micro-shrinkage defects, left hand) and in a post-solder joint (enormous porosity, right hand)**

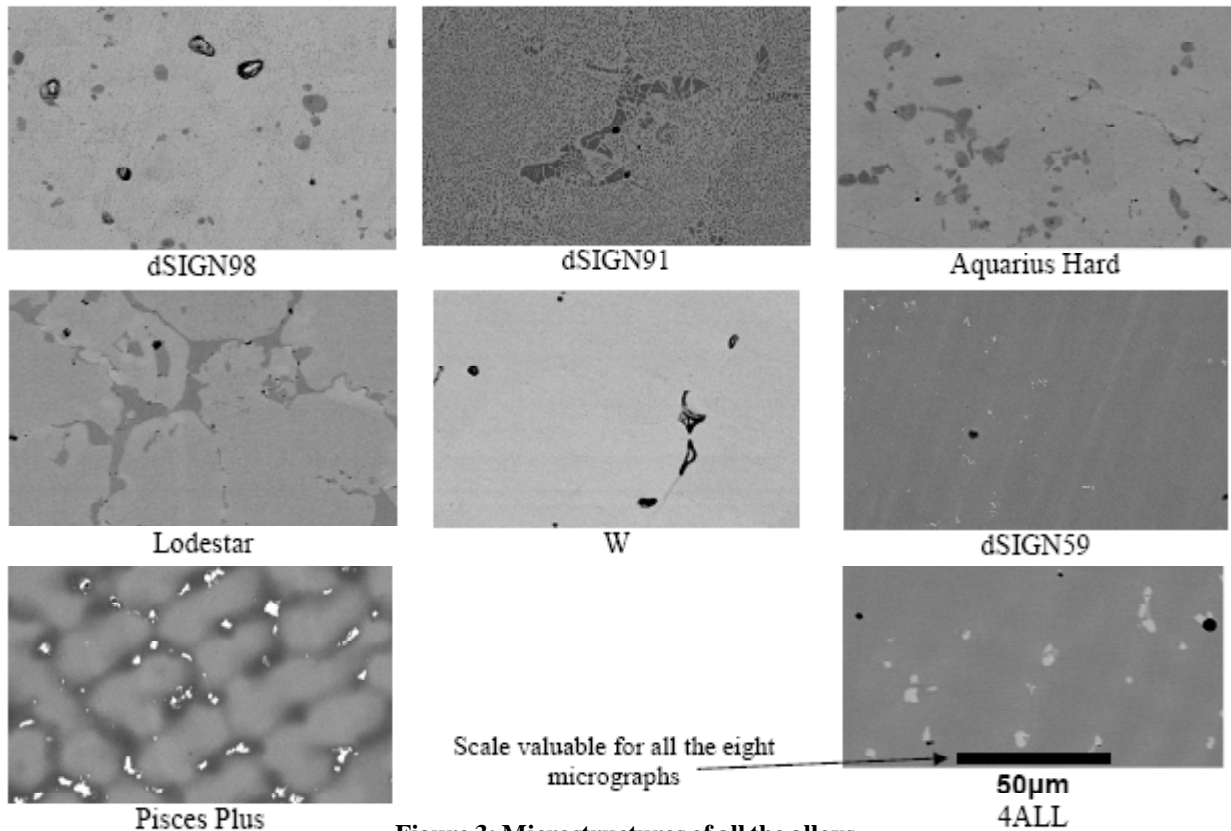


Figure 3: Microstructures of all the alloys

TABLE 6: Chemical compositions of the matrixes and the precipitates observed in several alloys and their pre-solder (I) and post-solder (II) joints (average values of 3 to 5 pinpoint WDS microprobe analyses)

dSIGN98	Au	Pt	Zn	In	Ta	Fe	Mn	Aquarius hard	Au	Pt	Pd	In	Ru	Ta	Fe	others	
Manufacturer's composition	85.9	12.1	2	<1	<1	<1	<1	Manufacturer's composition	86.1	8.5	2.6	1.4	<1	<1	<1	/	
Matrix(3 anal.)	79.29	10.31	1.36	0.09	0.00	0.07	0.06	Matrix (5 anal.)	86.39	4.64	2.28	1.44	0.06	0.00	0.52	0.33Ag	
Precipitates (3 anal.)	0.00	81.48	2.08	0.02	11.65	0.88	0.30	Precipitates (3 anal.)	0.00	74.38	1.43	0.18	4.18	15.49	2.16	0.11Ag	
(I) GPKF1015Y	Au	Ag	Pt	Sn	Zn	others		(I)HGPKF1015Y	Au	Ag	Pt	Sn	Zn	others			
Manufacturer's composition	60	36.5	<2.1	<1	<1			Manufacturer's composition	60	36.5	<2.1	<1	<1	/	/	/	
Matrix (3 anal.)	66.25	23.00	4.29	0.05	0.78	0.16Cu	0.02Fe	0.09Mn	Matrix (3 anal.)	65.37	27.55	2.68	0.10	0.34	0.43Pd	0.12Fe	0.04Ru
(II): .585	Au	Cu	Ag	Ga	Zn	others		(II): 0.650	Au	Cu	Ag	Ga	Zn	others			
Manufacturer's composition	58.5	18	16	7.2	<1			Manufacturer's composition	65	19.6	13	2	<1	/	/	/	
Matrix(3 anal.)	69.68	11.01	10.20	4.44	0.36	0.48Pt	0.08Sn	0.01Fe	Matrix (3 anal.)	73.93	11.87	8.70	1.30	0.15	1.00Pt	0.86Pd	0.56In
dSIGN91	Au	Pd	In	Ga	Ru	Re	others	others									
Manufacturer's composition	60	30.55	8.4	1	<1	<1											
Matrix (3 anal.)	57.13	26.25	8.56	1.13	0.01	0.00	8.56In	3.18Ag									
Precipitates (3 anal.)	48.21	27.70	11.58	2.12	0.06	0.00	0.08Cu										
(I): SHFWC	Au	Ag	Pd	In	Ru	others											
Manufacturer's composition	47	41	10.3	1.4	<1												
Matrix(3 anal.)	48.29	41.68	0	0.35	0.01	0.08Ga	0.07Cu	0.01Ru									
(II): 0.615	Au	Ag	Cu	In	Zn	others											
Manufacturer's composition	61.3	13.1	17.4	7.6	<1	/	/										
Matrix(3 anal.)	59.47	12.68	10.79	8.32	0.08	0.38Ga	0.02Re										

post-ceramic solders, while TABLE 6 displays some results of WDS analysis of matrix and precipitates in different types of alloys and solders.

Four alloys (dSIGN 98, dSIGN91, Aquarius Hard and Lodestar) present precipitates darker than matrix, because of the presence of higher contents of heavy elements in the matrix than in these precipitates. For instance, the total content of Au (resp. Au+Pt) is higher in matrix than in precipitates in the dSIGN91 alloy (resp. dSIGN98 and Aquarius Hard).

Inversely, precipitates are clearer than matrix for

## Full Paper

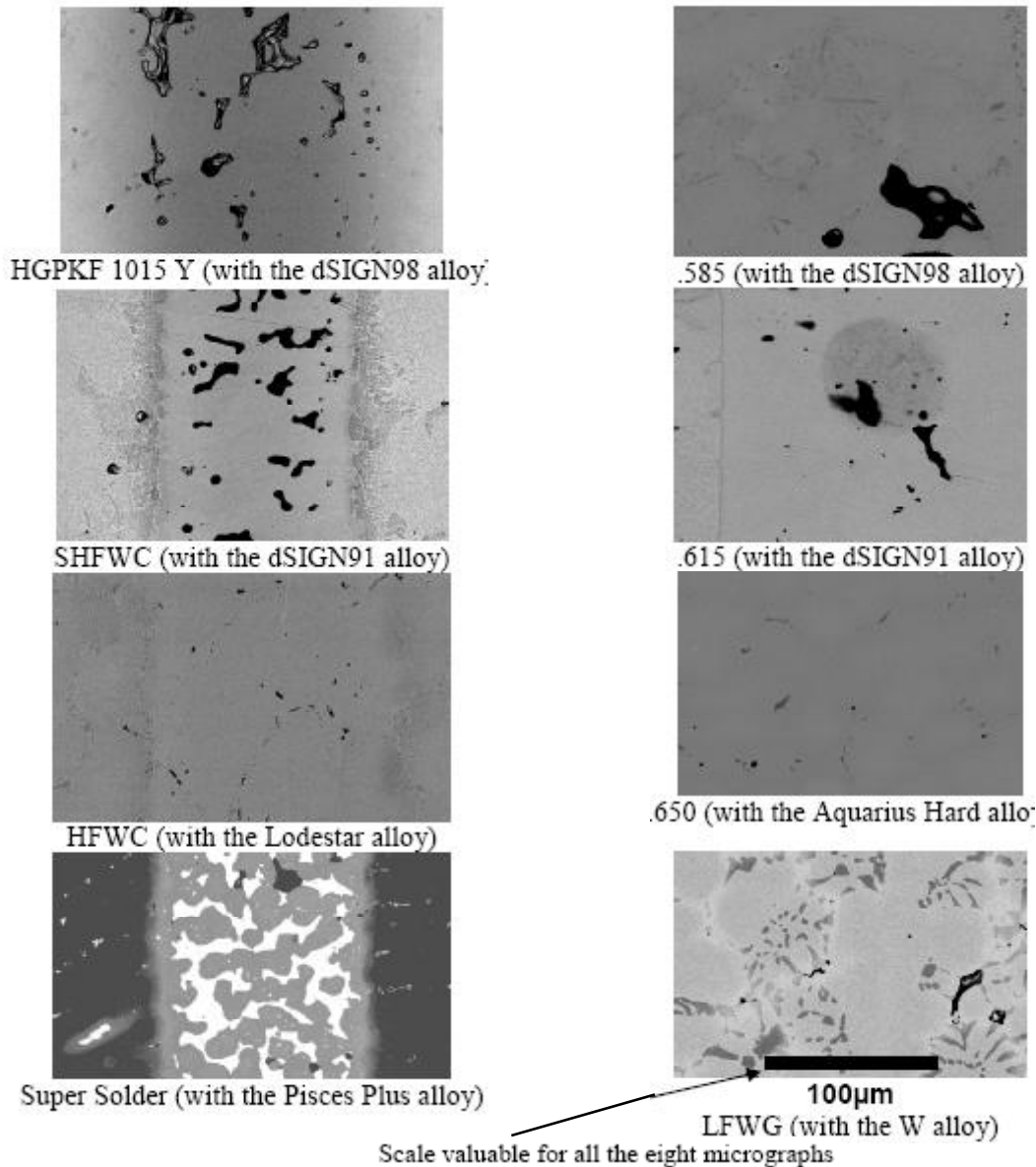


**Figure 4: Microstructures of the pre-solder (left hand) and post-solder (right hand) joints**

dSIGN59 and 4ALL, and are very white in Pisces Plus since they contain tungsten in a Ni-Cr matrix. For Pisces Plus, a dendritic structure is clearly visible, which could be related to a probable chemical segregation of light elements in the interdendritic areas during solidification. Dendrites outlines being diffuse, these alloys seem to contain no other phase in addition to the dendritic matrix and the clearly visible precipitates (which are noticeably rich in tungsten). W alloy appears as being only single-phased.

Some solders are often single-phased (HGPKF 1015 Y, SHFWC and 615) while others contain a small fraction of precipitates (HFWC, .585 and .650). On

the contrary, Supersolder and LFWC are clearly composed of two distinct phases with surface fractions that are of the same order of magnitude, especially Super Solder.

### Inter-diffusion areas

Figure 5 illustrates the inter-diffusion between solder and alloys. Its thickness is logically more important for pre-solders than for post-solders which are achieved at a lower temperature than the first ones. However, diffusions are always localized near the solder joint and do not concern the whole length of samples. From another way, the major thickness of the solder joint is not

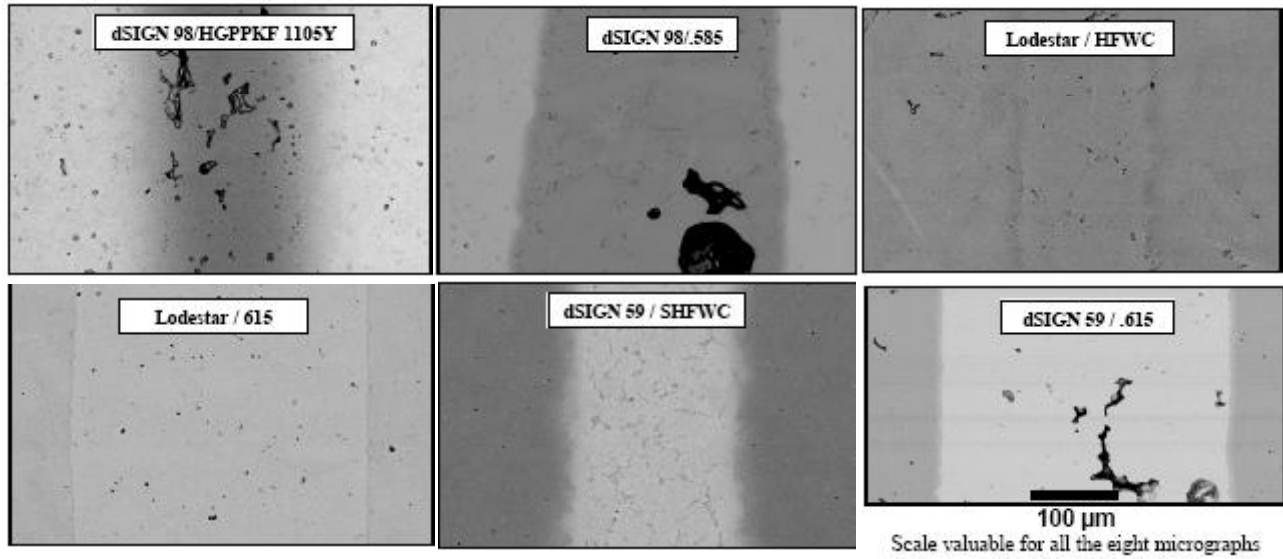


Figure 5: Examples of inter-diffusion zones between alloy and pre-ceramic solder joint (left) and between alloy and post-ceramic solder joint (right)

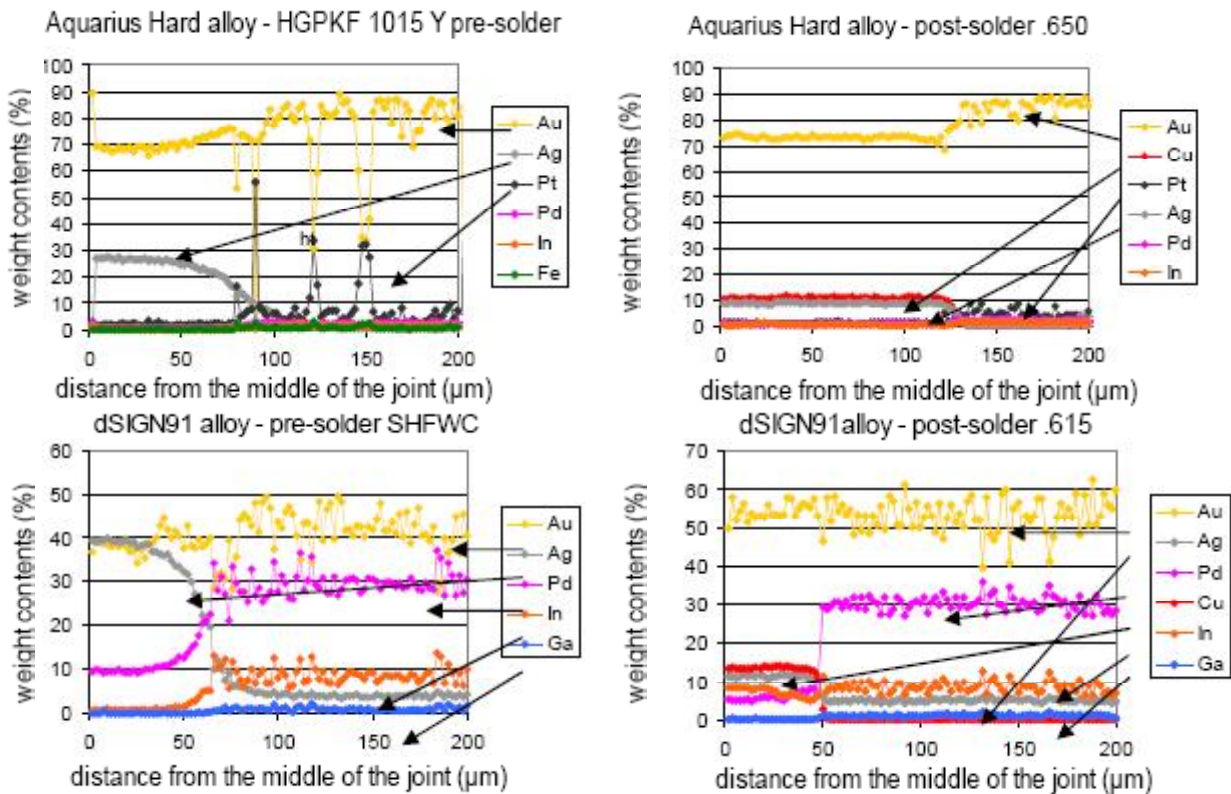


Figure 6: Concentration WDS profiles performed across the interdiffusion zone, for the Aquarius Hard and dSIGN91 alloys and their two types of solder

affected by diffusion of elements coming from the parent alloy. Figure 6 presents several concentration profiles performed from the middle of a joint towards the middle of the parent alloy (Aquarius Hard and dSIGN91), which allow to visualize the inter-diffusion

length with a better accuracy than microscope observations. For pre-ceramic solder, the zone of inter-diffusion is extended over about 50µm but chemical composition varies clearly only on half of this distance. For post-ceramic solder, this distance is at least two times

## Full Paper

less important and a difference between alloy and joint is more clearly seen.

### Vickers micro-hardness tests

Three  $Hv_{32g}$  micro-hardness measurements were performed on each parent alloy on the left and on the right of the solder joint, while three measurements were done on the solder joint itself (pre-solder or post-solder). The results present a good reproducibility, except for some solders in which porosities were embarrassing.

TABLE 7 presents the obtained results which show that the hardness values are quite different between parent alloys and their respective pre- and post-solders. Primary solders present about the same hardness as their parent alloys in half of situations, but are significantly lower for three couples. Inversely, secondary solders were harder than their parent alloys for three of them and lower for only one. The two Ni-Cr alloys (Pisces Plus and 4ALL) and W present equivalent micro-hardness with their respective pre-solder alloys. W presents the same hardness value for parent alloys and both pre-solder (HFWC) and post-solder (LFWG) alloys. This guarantees a good homogeneity of hardness all along of the framework of a fixed partial denture with the two types of solders. One can observe that a same alloy or a same solder alloy may present different hardness results depending on the type of assemblage (couple parent alloy-solder alloy).

### General commentaries

Different parts of framework sampled for this study present internal defects that could be identified as micro-shrinkage defects, very numerous in some of situations. Soldering two parts of parent alloy was sometimes delicate with in some cases the appearance of defects as void spaces. They can be gas-defects or lack of alimentation by liquid alloy. Such defects can decrease the mechanical resistance of the framework which cannot be always detected and known since there are internal defects that only a cut of the piece can reveal. This problem of internal healthy of solders is less important when two noble alloys are soldered with a noble soldering alloy or when a Predominantly Base alloy (Ni-Cr) is soldered with a less noble soldering alloy (Pd-Ni based).

Structural aspects of the different studied alloys are very variable. Some of them are single-phased and oth-

**TABLE 7: Values of vickers micro-hardness (32g) obtained for the alloys and solder joints**

Samples with pre-solder (I)		Samples with post-solder (II)	
Alloy	Pre-solder	Alloy	Post-solder
dSIGN98 (I)	HGPKF 1015Y	dSIGN98 (II)	0.585
186 +/- 13	51 +/- 10	145 +/- 7	164 +/- 11
dSIGN91 (I)	SHFWC	dSIGN91 (II)	.615
227 +/- 5	127 +/- 23	218 +/- 6	212 +/- 43
Aquarius hard (I)	HGPKF 1015Y	Aquarius hard(II)	0.650
89 +/- 11	74 +/- 10	104 +/- 5	167 +/- 17
Lodestar (I)	HFWC	Lodestar (II)	.615
226 +/- 12	198 +/- 15	233 +/- 7	170 +/- 25
W (I)	HFWC	W (II)	LFWG
161 +/- 12	155 +/- 12	165 +/- 7	166 +/- 22
dSIGN59 (I)	SHFWC	dSIGN59 (II)	.615
230 +/- 14	147 +/- 4	234 +/- 22	266 +/- 30
Pisces plus (I)	Super solder	Post-solder not realized	
268 +/- 13	261 +/- 4		
4ALL (I)	Super solder	Post-solder not realized	
212 +/- 12	195 +/- 30		

ers multi-phased. For this last case, a second phase can be intergranular (Lodestar) or interdendritic (Pisces Plus), under a spherical aspect with a homogeneous repartition (dSIGN 98), or both under an intergranular eutectic form and thin particles dispersed in the matrix (dSIGN 91), probably appeared by solid state precipitation. The soldering alloys can also present different structures which can be single-phased or multi-phased. The average atomic number of elements within the different phases allows to discriminate them when observed with the scanning electron microscope in back-scattered electrons mode.

Thermal cycles following or foregoing soldering step, as soldering procedure itself, are also different depending on the types of alloy and of solder realized. This can lead to different microstructures for a same composition of parent alloy or solder, and consequently to different values of hardness (and even mechanical properties from a general point of view).

The dSIGN98 alloy is harder when in a sample with its pre-ceramic solder than with its post-ceramic solder. This can be explained by the presence of more numerous gray blocky precipitates in the first sample compared to the second one. In other cases (dSIGN91, Aquarius Hard, W, dSIGN59), the hardness values are quite equal between the two types of respective soldering samples, since the microstructures are really similar. The Lodestar alloy, which presents an intergranular gray phase clearly more important in the pre-ceramic soldered sample, does not even present a significant difference of hardness with the post-ceramic sol-



dered sample. Pre-ceramic solder HGPKF 1015 Y is slightly harder when it solders Aquarius Hard alloys than when it solders dSIGN98, despite of the fact that its microstructure is similar. The presence of micro-shrinkage defects in the SHFWC pre-solder joint of dSIGN91 instead of the inter-granular gray phase seen with dSIGN59, leads to a slightly decrease in hardness. For pre-solder HFWC and Super solder, it is for the first one the presence of some precipitates and for the second one a different repartition between intertwined gray and white phases, that leads to a higher hardness for Lodestar and Pisces Plus samples compared to respectively W and 4ALL samples. For the .615 post-solder, which is used with three different parent alloys (dSIGN 91, Lodestar and dSIGN 59), the hardness values are rather different but it is difficult to explain this by microstructure observations.

Soldering and thermal cycles imply inter-diffusion which continues during the following firing. This leads to diffuse borders (pre-ceramic solder) or more delimited borders (post-ceramic solder). The importance of diffusion area can be evaluated by metallographic study since it is always well seen with SEM and by microprobe concentration profiles analysis. If alloy transition is clean-looking between parent alloy and post-ceramic solder, it is not too large for pre-ceramic solder joint and the original composition of solder alloy still exists in all situations between the two soldred pieces of parent alloy soldered. Thus, the framework of a final fixed partial denture can be a succession of several distinct materials: parent alloy-pre-solder alloy-parent alloy-post-solder alloy-parent alloy. This implies that mechanical characteristics could be not homogeneous along the complete framework as it was seen for hardness values. This can concern also others properties as corrosion resistance with a specific risk of local deterioration of framework by saliva in oral conditions by galvanic corrosion between solder and an element of parent alloy, for example.

## CONCLUSIONS

The conception and realization of a framework for ceramic-metal fixed partial denture implies alloys and solders which can present different properties and behavior from both the metallurgical and the microstructure points of view. The mechanical properties of a

framework can be considerably affected during the service-life of the prosthesis. Many other factors can also dramatically affect the mechanical resistance of the ceramic-metal prostheses, like local corrosion phenomena since the framework is often not entirely coated by cosmetic ceramic and some parts can be exposed to oral corrosive environment.

## ACKNOWLEDGMENTS

The authors gratefully thank the firm Ivoclar-Vivadent who provided them all alloys and solders they needed, and the Common Service of Micro-analysis of the Faculty of Science and Techniques of the University Henri Poincare Nancy 1, for its contribution to this work.

## REFERENCES

- [1] J.Philibert, A.Vignes, Y.Brechet, P.Combrade; 'Metallurgie : du Minerai au Matériau', 2<sup>nd</sup> Edition, Dunod, Paris, (2002).
- [2] J.B.Schwartz; 'Brazing for the Engineering Technologist', Chapman and Hall, London, (1995).
- [3] B.E.Schiffleger, G.J.Ziebert, V.B.Dhuru, W.A.Brantley, K.Sigaroudi; J.Prosthet.Dent., **54**, 770 (1985).
- [4] G.J.Ziebert, A.Hurtado, C.Glapa, B.E.Schiffleger; J.Prosthet.Dent., **55**, 312 (1986).
- [5] S.Schluger, R.A.Youdelis, R.C.Page, R.H.Johnson; 'Periodontal Diseases', Leaand Febiger, Philadelphia, (1990).
- [6] L.Wictorin, H.Fredriksson; Odontol.Revy., **27**, 187 (1976).
- [7] R.Kriebel, B.K.Moore, C.J.Goodacre, R.W.Dykema; J.Prosthet.Dent., **51**, 60 (1984).
- [8] H.W.Wiskott, J.I.Nicholls, R.Taggart; J.Dent.Res., **70**, 140 (1991).
- [9] T.J.Butson, J.I.Nicholls, T.Ma, R.J.Harper; Int.J.Prostodont, **6**, 468 (1993).
- [10] H.W.Wiskott, J.I.Nicholls, U.C.Belser; Dent.Mater., **10**, 215 (1994).
- [11] E.B.Hawbolt, M.I.MacEntee; J.Dent.Res., **62**, 1226 (1983).
- [12] H.W.Wiskott, F.Macheret, F.Bussy, U.C.Belser; J.Prosthet.Dent., **77**, 607 (1997).
- [13] L.M.Willis, J.I.Nicholls; J.Prosthet.Dent., **43**, 272 (1980).